E-ISSN: 2707-6644
P-ISSN: 2707-6636
IJCPDM 2022; 3(2): 52-58
Received: 15-04-2022
Accepted: 25-06-2022

Obaje Samuel Enemakwu
Department of Computer Engineering, Federal Polytechnic, Offa, Nigeria

Corresponding Author:
Obaje Samuel Enemakwu
Department of Computer Engineering, Federal Polytechnic, Offa, Nigeria

Effects of fingerprint recognition algorithms on toeprint and fingerprint

Obaje Samuel Enemakwu

DOI: https://doi.org/10.33545/27076636.2022.v3.i2a.70

Abstract
Democracy is a form of government in which politicians are chosen by popular vote. Voting may be done using behavioural biometrics, known as transparent balloting, which involves indicating a candidate of preference by indication, or physiological biometrics, known as hidden balloting, which involves appending a fingerprint to a vote. In certain countries around the world, fingerprints are used to cast ballots. However, injury casualties, natural disaster victims, and lepers, who account for one out of every 10,000 people in the world's population of approximately 7.7 billion, may pose a concern if their fingerprints are used to classify them. Two photographs were chosen to make up the sample collection: a Toeprint image with a left loop to be contrasted with a fingerprint image with a left loop. The photos were subjected to the standard fingerprint recognition algorithm, which included processes such as Normalisation, Orientation, Binarization, Thinning, and Minutiae Extraction. Since the experiment was not designed to measure the accuracy of the recognition algorithm, processing time and image quality were not taken into account. When the findings were compared, it was discovered that the algorithm had the same impact on both photos and that the derived minutiae points, which are the foundation for successful matching, were greater than 100. A modern method of self-identity and voting for lepers and injury patients is now accessible.

Keywords: leprosy, minutiae extraction, left loop, matching, toeprint, fingerprint, democracy, ballot, elected, voting

1. Introduction

Democracy is a democracy in which the citizens of its territory by-elections directly or indirectly rule. The international human rights community frowns on any dictatorship somewhere in the world that does not practice democracy. That allows me to state unequivocally that democracy is the order of the day in the vast majority of the world's countries. Election refers to selecting a chief or other official by popular voting. Voting is the act or instance of engaging in such a decision by submitting a vote.

Voting may be done by "open balloting," through which Behavioral Biometrics such as lifting hands or appending an indicator by dropping on the row behind a candidate of preference is used. Alternatively, "hidden balloting," in which voting is achieved by appending the fingerprint to a preference nominee space on the ballot paper, is a Physiological Biometric. Recently, an automatic voting scheme has been implemented in which the fingerprint is appended directly to an accreditation hand-holding gadget.

For some years now, the fingerprint has become the primary form of voting in an appropriate democratic environment all over the planet. It is painful to mention that since leprosy patients lack fingerprints, they cannot vote in this mode. According to WHO (2017) [11], there is 1 leprosy survivor for every 10,000 people in the world's population of 7.7 billion, as revealed by the United Nations in Worldometer (2019) [10]. This vast number of lepers, a stigmatised community of individuals, are not celebrating democracy at all. In order to reintroduce this group of individuals into the electoral structure, their Toeprint should be able to substitute the fingerprint easily.

2. Literature Review

Toe printing is the act of creating an image of the papillary Ridge of the toes for identifying purposes. While dactylics have not studied the Toeprint extensively, it is clear that the toe, like the fingers, has ridges that could be tested. Sir Francis Galton, an English physicist interested in heredity, is said to have amassed the first large number of fingerprint data late in the nineteenth century.

After extensive investigation, he identified the two fundamental facts on which fingerprint recognition is based: one, the ridge arrangement on every finger of every individual is distinct, and two, the ridge arrangement stays constant throughout one's existence. This evidence may be traced back to previous studies, but they could not come to such a firm conclusion as this. According to (Obaje and Ibiyemi, 2010) [8], the toes have identical features to fingerprints and may also be used for personal recognition. Fig 1 depicts the division of toeprints.

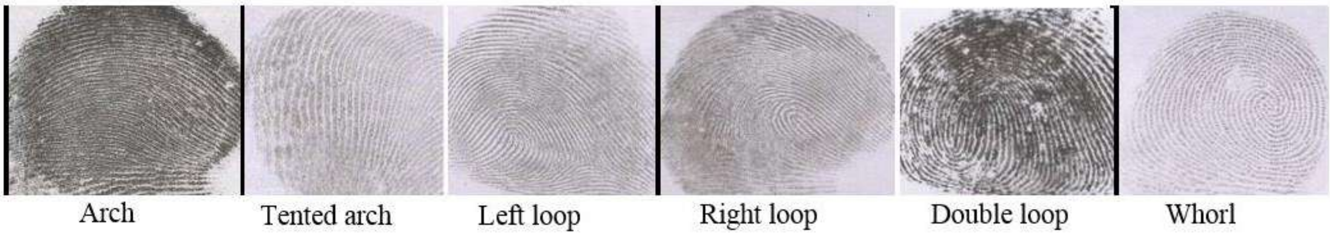

Fig 1: Sample Toeprint Classification

The positional name is used to identify the digits. For example, the thumb is the smallest and thickest finger that stands separately from the other four, preceded by the index, centre, ring, and eventually the little. We still have the five toes. As seen in Fig. 1, these are the main toe, the index toe, the middle toe, the fourth toe, and the little toe. Middle, ring and finally, the little. Also, we have the five toes as shown in fig 2.

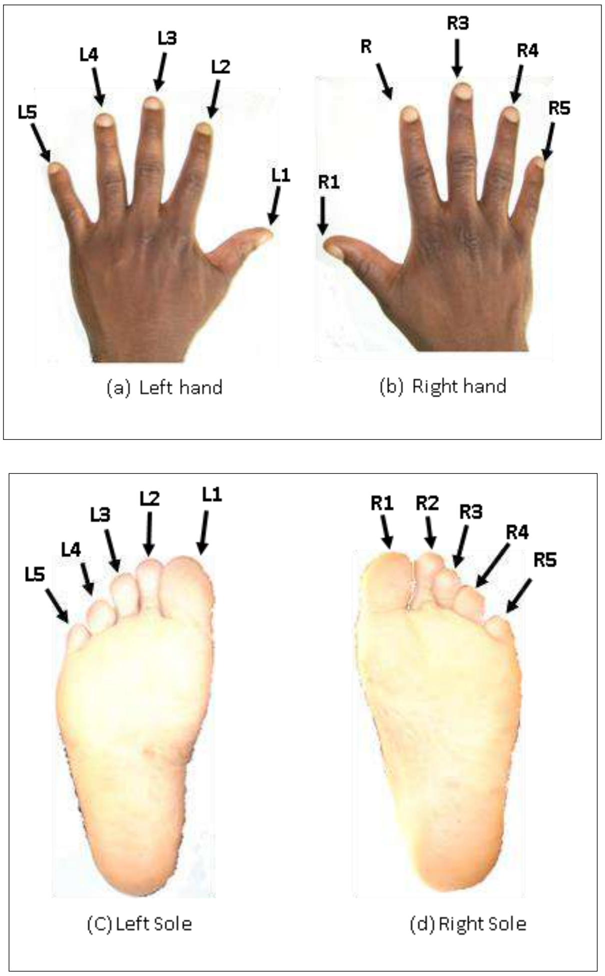

Fig 2: The Comparison of Fingerprint and Toeprint by name

Key to Fig. 2

(a) Left Hand (L1 = Thumb, L2 = Index, L3 = Middle, L4 = Ring, L5 = Little)
(b) Right Hand (R1 = Thumb, R2 = Index, R3 = Middle, R4 = Ring, R5 = Little)
(c) Left Sole (L1 = Big Toe, L2 = Index Toe, L3 = Middle Toe, L4 = Fourth Toe,
L5 = Little Toe)
(d) Right Sole (R1 = Big Toe, R2 = Index Toe, R3 = Middle Toe, R4 = Fourth Toe,
R5 = Little Toe)

The experiment's aim is to apply the fingerprint recognition algorithm to Toeprint to see if the results are the same as those obtained by applying the same algorithm to the fingerprint. To do this, the sample collection was deliberately chosen, meaning that both the Toeprint and fingerprint used belonged to the same class, the left loop.

3. Materials and Method

The fingerprint recognition algorithm (Jain *et al.*, 2020; Chandan *et al.*, 2020; Zhang, 2020; Hong, Wan, and Jain, 2019; Maltoni *et al.*, 2021) [4, 2, 12, 3, 5] was used to evaluate both the Toeprint image and a reference fingerprint image for comparison purposes.

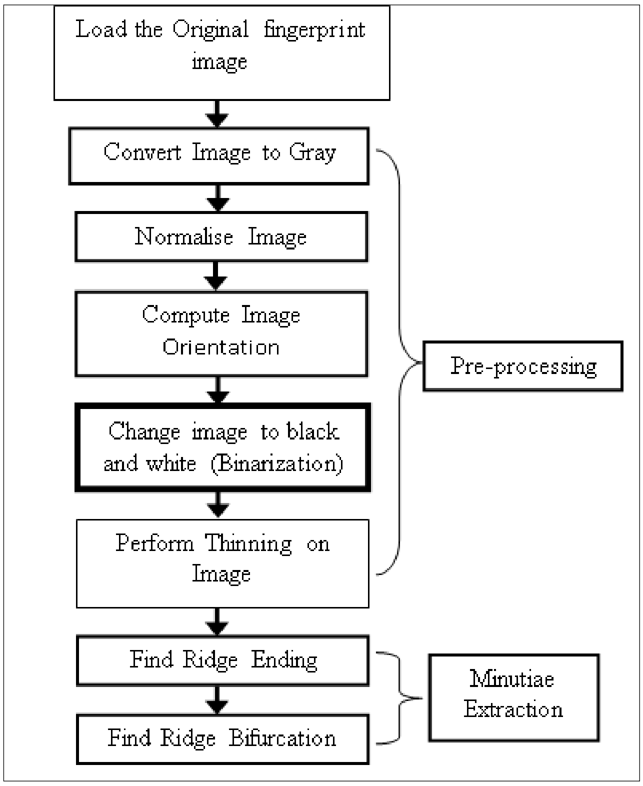

Fig 3: Pre-processing and Minutiae Extraction Flowchart

3.1 Using fingerprint recognition algorithm on toeprint image

Pre-processing is important since fingerprint or toeprint images are acquired using either the ink dab system or sensors which include ambiguities due to incorrect finger/toe pressure or other noise sources, lowering the quality of the images obtained. This may be a major issue in function extraction and matching systems. To improve image consistency, pre-processing must be performed prior to function extraction. Various methods for image enhancement are possible, as stated in (Jain *et al*., 2020; Chandan *et al*., 2020; Zhang, 2020; Hong, Wan, and Jain, 2019; Maltoni *et al*., 2021) [4, 2, 12, 3, 5], but the best approach depends on the quality of the image.

Pre-processing of fingerprint images requires segmentation–separating the backdrop and foreground to eliminate false minutiae. This is also known as ROI extraction. (ii) Image enhancement-to increase image contrast, lighting, and quality; and (iii) Binarisation-to achieve a strong contrast between ridges (black) and valleys (white) (white).

The image enhancement of fingerprint images may be accomplished using one of the following methods or a mixture of these methods; in this experiment, the flowchart was used in the measures shown in Fig. 3.

3.1.1 Histogram Equalisation

An image's histogram reflects the relative frequency of the image's different gray levels. It is a technique for improving picture contrast by changing the strength of each gray level in the image. A stronger outcome is obtained by histogram equalisation with adaptive threshold keeping.

Follow the measures below to perform Histogram Equalisation on the files.

Using the method, calculate the equalised cumulative frequency;

$$C_K = \left\{\left[\sum_{j=0}^{K} hist(j)\right] \cdot \left[\frac{L}{MN}\right]\right\} + 0.5 \quad \dots\dots..(1)$$

Remap the intensities of the initial grey picture to the intensities of the equalised image;

$$E^{'''}(X,Y) = C\,[E^{''}(X,Y)]\ , X = 0,1,\dots\dots N; Y = 0,1,\dots\dots, M-1 \quad \dots.(2)$$

3.1.2 Filtering approach

Various filtering approaches may be used to improve the quality of a fingerprint file. Any filters that may be found in fingerprints tainted by noise are the wiener filter, median filter, high pass filter, and so on. Another useful strategy is the Gabor filter, which improves the contrast between the foreground ridges and the horizon.

For the enhancement of the low-quality images in this work, the approach suggested in (Hong, Wan, and Jain, 2019) [3] based on Gabor filters was selected. Gabor filters have both frequency and orientation selectivity and joint optimal resolution in both the spatial and frequency domains.

The Gabor filter was built using the even-symmetric actual portion of the original 2D Gabor filter, which was also used (Hong, 2019) [3]. Consequently,

$$g(x,y,T,\varphi) = exp\left(-\frac{1}{2}\left[\frac{x_\varphi^2}{\sigma_x^2} + \frac{y_\varphi^2}{\sigma_y^2}\right]\right) cos\left(\frac{2\pi x_\varphi}{T}\right) \quad (3)$$

$$x_\varphi = x\cos\varphi + y\sin\varphi \quad (4)$$

$$y_\varphi = -x\sin\varphi + y\cos\varphi \quad (5)$$

Where φ is the direction of the derived Gabor filter and T is the sinusoidal plane wave period.

The following formula can be deduced by dividing the equation into two orthogonal components, one parallel and one perpendicular to the orientation φ.

$$g(x,y,T,\varphi) = h_x(x;T,\varphi)\ X\ h_y(y;\ \varphi)$$

$$= \left\{exp\left(-\frac{x_\varphi^2}{2\sigma_x^2}\right) cos\left(\frac{2\pi x_\varphi}{T}\right)\right\}.\left\{exp\left(-\frac{y_\varphi^2}{2\sigma_y^2}\right)\right\} \quad (6)$$

The first component, *hx*, is a 1-D Gabor function that acts as a bandpass filter, and the second part, *hy*, is a Gaussian function that acts as a low pass filter.

Φ Finally, a 2D even-symmetric Gabor filter (TGF) conducts low pass filtering along its orientation and bandpass filtering orthogonal to its orientation φ.

3.1.3 Normalisation

Image normalisation is a common technique for image enhancement. It is a pixel-by-pixel process used for intensity correction, with the key goal of reducing differences in gray-level values between ridges and valleys. The pictures can be normalised.

$$F^{''}(X,Y) = \begin{cases} \mu_0 + \dfrac{\sqrt{\sigma_0^2 .(F^{'}(X,Y)-\mu)^2}}{\sigma^2} & ,if\ F^{'}(X,Y) \geq \mu \\ \mu_0 - \dfrac{\sqrt{\sigma_0^2 .(F^{'}(X,Y)-\mu)^2}}{\sigma^2} & ,otherwise \end{cases} \quad \dots\dots(7)$$

$$Where\ \mu_0 = 100 \Rightarrow desired\ to\ mean;\ \sigma_0 = 100 \Rightarrow desired\ variance$$

3.1.4 Local Ridge Orientation

The orientation is the angle created by the horizontal line and the ridge inclination. Orientation is calculated on a block-by-block basis rather than a pixel-by-pixel basis. Rao's latest hierarchical method, proposed in 2021, divides the picture into w x w blocks, then uses the measured *gx* and *gy*, gradients, calculated centred at pixel (*i*,*j*), and the provided equations. These blocks are either 8 or 1616 pixels in size. The steps are:

(a) Divide the image into *w* x *w* overlapping blocks. The window size is taken as 8x 8.

(b) The gradients *Vx* and *Vy* are computed using the Sobel filter. *Vx* represents the horizontal gradient component, and V*y* represents the vertical gradient component.

(c) The average gradient vectors are computed as follows:

$$Vx(i,j) = \sum_{u=i-8}^{i+8} \sum_{v=j-8}^{j+8} 2gx(u,v)gy(u,v),$$

$$Vy(i,j) = \sum_{u=i-8}^{i+8} \sum_{v=j-8}^{j+8} gx^2(u,v) - gy^2(u,v), \quad (8)$$

(d) Direction Estimation

$$\theta(i,j) = \frac{1}{2} archtan\left(\frac{Vy(i,j)}{Vx(i,j)}\right) \quad (9)$$

The quiver plot is used to build the path diagram, and the orientation picture is stored.

3.1.5 Binarisation of Image

Separate the Ridge from the Furrow (Valley) such that the minutiae points may be rendered unique by the Binarization method.

Using the form suggested in (Peihao *et al* 2007) [13], picture binarisation classifies each pixel as a "ridge" (darker) or "valley" (lighter) (lighter). Using the following principles, we add a binarisation procedure to an improved picture B *(i, j).:*

a) Assign "ridge' to pixel *(i, j)* if $B(I, j) \leq Pk$, where *Pk* is the *Kth* percentile of histogram of {*B(i,j)*}, e.g. *k* = 25 in this case.

b) Assign "valley" to pixel (i, j) if $B(i, j). \geq P_{50}$,

c) The remaining pixel {(I, j)} are classified as "valley" if $B(i, j) \geq T_{5x5}$, and 'ridge" otherwise; where T_{5x5} is the 30^{th} percentile of 5x5 pixel values surrounding the pixel (i, j).

3.1.6 Thinning

Finding the skeleton of the binarised image via the Thinning procedure is a critical stage in the preprocessing. It makes it easy to find the Minutiae points.

The thinning algorithm mentioned by Zhang and Suen (2020) [12] was used in this case.

The system consists of consecutive passes of two simple measures added to the region's contour points. A contour point p0 is described as having at least one background pixel in its 8-pixel neighbourhood. If any of the following criteria apply to a contour point's 8-pixel neighbourhood, it is labelled for deletion in the first pass.

a) The region's neighbours would have 2 to 6 neighbours.

b) All background-neighbouring neighbours must be connected.

c) p2, p4 or p6 should be in the context

d) p4, p6 or p8 should be in the context

If all of the criteria are satisfied, the point is designated for deletion. To guarantee that the data structure is not updated during the step's implementation, the point is not discarded before all area points have been processed.

The first two conditions must always hold for a point to be marked for deletion in the second pass of the algorithm, but conditions (c) and (d) are modified as follows.

(c') p2, p4 or p8 should be in the context

(d') p2, p6 or p8 should be in the context

In short, the algorithm adds the following measures iteratively until only the skeleton of the field remains.

1. Phase one involves marking all bottom-right contour points for deletion.
2. Delete all contour points that have been labelled.
3. Stage two involves marking all top-left contour points for deletion.
4. Delete all contour points that have been labelled.

P8	P1	P2
P7	P0	P3
P6	P5	P4

.... (10)

The following equation (7) positions are being considered;

P0 = (*x*, *y*). p1= (*x*, *y*-1). P2 = (*x*+1, *y*-1). P3 = (*x*+1, *y*). p4 = (*x*+1, *y*+1). P5 = (*x*, *y*+1). P6 = (*x*-1, *y*+1). P7 = (*x*-1, *y*). p8 = (*x*-1, *y*-1) ....(11)

Occasionally, ridge boundary aberrations trigger hairy growth (spikes or line fuzz), contributing to spurious or artificial ridge ends and bifurcation. To restrict this, adaptive morphology filtering is needed (Fitz and Green, 1996) [14] for spike removal after thinning, and this process is referred to as 'pruning' (Jain *et al*, 1995) [15]. 'Dilation' is often a method of filling holes left from previous pre-processing operations. Post-processing methods focused on basic structural considerations are often used to remove much of the false minutiae that commonly impact thinning binary fingerprint pictures. The end of the pre-processing stage is marked by thinning.

3.2 Minutiae Point Detection

Detection of minor flaws the final stage of the binarisation process can be accomplished in this manner by using the method suggested by Bansal, Briti, and Punam (2011) [1]: Each ridge pixel in a thinned picture is grouped into one of the following groups based on its 8-connected neighbour. A ridge pixel is referred to as

(a) It is considered isolated if it has no 8 related neighbours.

(b) If it has only one 8-connected neighbour, it is an ending.

(c) If it has two 8-connected neighbours, it is an edge point.

(d) If it has three 8-connected neighbours, it is a bifurcation.

(e) It is a crossing if it has four 8-connected neighbours.

The crossing number technique was used to remove minutiae. In the equation, the crossing number of pixel 'p' is specified as half the total of the differences between pairs of adjacent pixels representing the 8-neighbourhood of 'p' (12).

$$C_N(p) = \frac{1}{2}\sum_{i=1....8} |val(p_{i\,mod\,8}) - val(p_{i-1})| \quad (12)$$

Where p0 to p7 are pixels in an ordered series that define p's 8-neighborhood and *Val* (p) is the pixel value.

4. Results and Discussion

4.1 Implementation Environment

Many of the methods and algorithms mentioned in this paper were implemented on the Windows 7 operating system using MATLAB R2015b. The tests were carried out on a Pentium (R) 2.20 GHz processor with 2.00 GB of RAM.

The Toeprint picture used in the experiment is one of 1183 healthy Toeprints taken from 140-person lepers at Nigeria's nine leprosariums. The TET Fund study grant I recently received allowed me to gather data (2014). Moreover, as part of the study activities, I must publish globally.

The fingerprint picture used in the experiment was derived from a previous study I completed as part of my PhD studies at the University of Ilorin in 2010. Both photographs were captured using the ink dab process.

Each picture is an 8-bit grey-level image scanned at approximately 600 dpi resolution and 256 X 256 pixels in size; the image format is a bitmap image compression algorithm. Even though the image size was not precisely 256 X 256, the software demanded that it be changed to this. This experiment aims to demonstrate that a comparable result will be obtained when the Toeprint is subjected to the same treatment as the fingerprint recognition algorithm. The influence of the algorithm on the Toeprint and the contrast of this effect with a related Fingerprint became the experiment's focus, rather than picture quality or execution speed.

Fig 4a: Toe Print Image

Fig 5a: Fingerprint Image

Fig 4b: Grayscale Toe Print

Fig 5b: Grayscale Fingerprint

Fig 4c: Normalized Toe Print

Fig 5c: Normalized Fingerprint

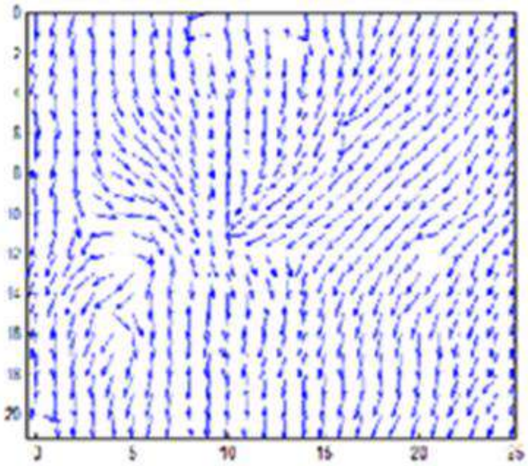

Fig 4d: Toe Print Orientation

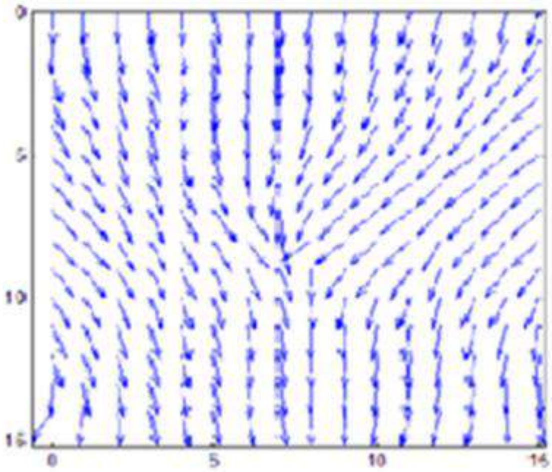

Fig 5d: Fingerprint Orientation

Fig 4e: Toe Print Binarization

Fig 5e: Fingerprint Binarization

Fig 4f: Toe Print Thinning

Fig 5f: Fingerprint Thinning

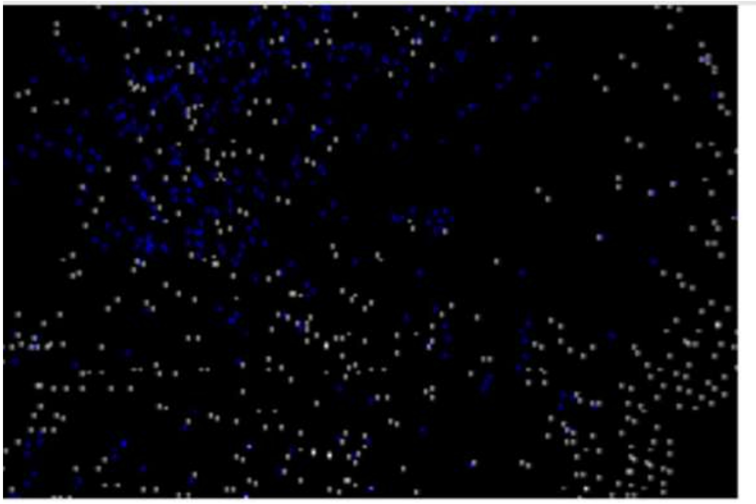

Fig 4g: Toeprint Minutiae Points: ending = white, bifurcation = blue

The experiment sample collection included Fig. 4(a) Original Toeprint picture–Left loop and Fig. 5(a) Original Fingerprint image–Left loop. The outcomes of the preprocessing and minutiae extraction processes conducted on the Original Toeprint picture (Fig. 4(a)) are as follows: 4(b) Grayscale, 4(c) Normalisation, 4(d) Orientation, 4(e) Binarisation, 4(f) Thinning, and finally 4(g) Minutiae 3 Extraction. The fingerprint in Fig. 4(b) through 4(g) experienced the same thing, allowing it to be linked to the contribution of the Toeprint. The thinning (image skeleton or 1 pixel thick) result for the Toeprint shown in 4(f) is clearer than the fingerprint result shown in Fig. 5(f). The inconsistency in results is attributed to image quality and thresholding problems, which may have been addressed if further attention had been paid to the algorithm. A successful thinning process would enable us to obtain more precise minutiae points. Since the two photographs (Toe and Fingerprint) were of the same class, the lines of orientation in Fig 4(d) and 5(d) seem close (Left loop). The Minutiae points obtained for both the Toeprint and fingerprint in Fig 4(g) and 5(g) were found to be greater than 100, proving that (Moenssens, 2020) states that a high-quality fingerprint usually comprises between 40 and 100 minutiae. As a result, the Toeprint will easily substitute the fingerprint for lepers and injured patients who cannot vote due to a lack of a fingerprint.

5. Conclusion

The experiment showed that, like the fingerprint, the Toeprint has the essential characteristics of being peculiar to individuals, having patterns that can yield minutiae marks, and therefore can be used to distinguish and recognise a person completely. A modern form of personal authentication known as the Toeprint is proposed here, capable of being used for voting for lepers and injury patients who do not have a fingerprint.

6. Acknowledgements

My heartfelt gratitude goes to the TET Fund, Tertiary Education Trust Fund, in Nigeria, which funded my study on the topic through the National Research Fund scheme.

7. References

1. Bansal R, Priti S, Punam B. Minutiae extraction from fingerprint images-A Review. arXiv preprint arXiv; c2011. p. 1201.1422.
2. Chandan S, Mihir M. DSP Implementation of Fingerprint-Based Biometric System, Part iv Project Final Report, Department of Electrical & Computer Engineering, The University of Auckland; c2020.
3. Hong L, Wan Y, Jain A. Fingerprint Enhancement Algorithms and Performance Evaluation, IEEE Trans. On pattern, Analysis and Machine Intelligence. 2019;20(8):777-789.
4. Jain K, Hong L, Pankanti S, Bolle R. Online Fingerprint Verification, IEEE transaction Pattern Analysis & Machine Intelligence. 2020;19(4):302-313.
5. Maltoni D, Maio D, Jain AK, Prabhakar S. Handbook of Fingerprint Recognition, Springer, New York; c2021.
6. Moenssens A. Fingerprint Techniques, Chilton Book Company, London; c2020.
7. Obaje SE. Lepers Personal Identification Using the Soleprint in Place of Fingerprint. Paper delivered at the 3rd International Conference on Electronics and Computer Technology, Kanyakumari, India; c2011. p. 8-10.
8. Obaje SE, Ibiyemi TS. Automatic Fingerprint and Toeprint Recognition for Personal Identification and Forensic Application. Final Report, Department of Electrical & Electronics Engineering, University of Ilorin; c2010.
9. Rao AR. A Taxonomy for Texture Description and Identification, Springer, New York, NY; c2021.
10. Worldometer. World Population Clocks 7.7 Billion People; c2019. www.worldometer.info
11. WHO. Fact Sheet on Leprosy, Disabled People International. United Nations Enable; c2017. www.un.org.
12. Zhang TY, Suen CY. A Fast Parallel Algorithm for Thinning Digital Patterns, Communications of ACM. 2020;27(3):236-239.
13. Xu Pei, Peng Peihao, Wang Yukuan. Estimation and assessment on eco–water storage of the Jiuzhaigou Natural Reserve. Earth and Environment. 2007;35(1):61-64.
14. Fitz AP, Green RJ. Fingerprint classification using a hexagonal fast Fourier transform. Pattern recognition. 1996;29(10):1587-1597.
15. Jain R, Kasturi R, Schunck BG. Machine Vision, McGraw-Hill, Inc, USA; c1995.